

## Measurement of the neutron-neutron scattering length $a_{nn}$ with the reaction $\pi^-d \rightarrow nn\gamma$ in complete kinematics

O. Schori,\* B. Gabioud,\* C. Joseph, J. P. Perroud, D. Rügger, and M. T. Tran  
*Institut de Physique Nucléaire, Université de Lausanne, CH-1015 Lausanne, Switzerland*

P. Truöl and E. Winkelmann†  
*Physik-Institut, Universität Zürich, CH-8001 Zürich, Switzerland*

W. Dahme  
*Sektion Physik, Universität München, D-8046 Garching, Federal Republic of Germany*  
(Received 30 December 1986)

The neutron-neutron scattering length  $a_{nn}$  is determined from the low energy part of the neutron spectrum of the reaction  $\pi^-d \rightarrow nn\gamma$  with pions at rest. Since neutrons are detected in coincidence with the photon, the kinematics is completely determined. We obtain  $a_{nn} = -18.7 \pm 0.6$  fm, in agreement with a result of a previous experiment based on the analysis the photon spectrum.

### I. INTRODUCTION

Since 1954, when Phillips and Crowe<sup>1</sup> performed the first measurement of the reaction  $\pi^-d \rightarrow nn\gamma$  and demonstrated that the neutron-neutron interaction at low energies is attractive and a bound dineutron does not exist, the determination of the low energy neutron-neutron scattering parameters continues to be a controversial and debated issue. The controversy arises from the observation that the analysis of the four most recent kinematically complete experiments for the deuteron breakup process  $nd \rightarrow pnn$  yields an average value of  $a_{nn} = -16.8 \pm 0.4$  fm,<sup>2-5</sup> while our own, hitherto most precise experiment on  $\pi^-d \rightarrow nn\gamma$ , yielded  $a_{nn} = -18.5 \pm 0.4$  fm.<sup>6</sup> The debate centers on the difference between  $a_{nn}$  and the Coulomb corrected proton-proton scattering length  $a_{pp}$ . Such a difference would, of course, signal charge symmetry violation, which is expected on the basis of  $\rho$ - $\omega$  mixing<sup>7</sup> or, more fundamentally, on the basis of the mass difference between the  $u$  and  $d$  quarks<sup>8</sup> and appears also in the  ${}^3\text{H}$ - ${}^3\text{He}$  binding energy difference. A typical prediction is  $|a_{pp}| - |a_{nn}| = -0.9$  fm,<sup>7</sup> which is supported experimentally by our measurement of  $a_{nn}$  and the "recommended" value of  $a_{pp} = 17.3 \pm 0.2$  fm,<sup>9</sup> but in disagreement with the  $nd \rightarrow pnn$  value.

Further points which have stimulated the discussion are the following:

(i) There is a significant difference between the average value of  $a_{nn}$  taken from kinematically complete experiments for  $nd \rightarrow pnn$  and other reactions involving three hadrons in the final state such as  ${}^3\text{H}d \rightarrow {}^3\text{H}enn$  or  ${}^3\text{H}t \rightarrow {}^4\text{H}enn$  ( $\bar{a}_{nn} = -16$  to  $-17$  fm) or from the kinematically incomplete experiments ( $\bar{a}_{nn} = -18$  to  $-24$  fm).

(ii) There is a difference between neutron pick-up ( $\bar{a}_{nn} = -16.7 \pm 0.5$  fm) and proton knock-on processes ( $\bar{a}_{nn} = -20.7 \pm 2.0$  fm) studied in different kinematical regions of  $nd \rightarrow pnn$ .

(iii) The latter difference is interpreted as evidence for three body forces,<sup>10</sup> which, in turn, would also resolve the discrepancy between the  $\pi^-d \rightarrow nn\gamma$ , and  $nd \rightarrow pnn$  data, i.e., only  $\pi^-d \rightarrow nn\gamma$  yields  $a_{nn}$  directly.

(iv) Though the reaction  $\pi^-d \rightarrow nn\gamma$  seems clearly preferred since only a photon is present with the two neutrons in the final state, a measurement of the photon spectrum, as in our previous experiment, does not completely determine the kinematical situation.

(v) In radiative pion capture the consequences of the various assumptions entering the theoretical model needed to extract  $a_{nn}$  from the data were evaluated and the uncertainty is included in the error quoted,<sup>6</sup> while this was not done for the hadronic reactions.

(vi) The only other  $\pi^-d \rightarrow nn\gamma$  experiment<sup>11</sup> with a reasonably small error in the result obtained  $a_{nn} = -16.7 \pm 1.3$  fm from an analysis of the  $nn$ -angular correlation and the neutron energy spectrum taken in coincidence with a photon.

Though we had convincingly argued in favor of using  $\pi^-d \rightarrow nn\gamma$  over purely hadronic reactions, if the  $nn$ -scattering parameters are to be determined, and furthermore our previous experimental result properly defended, we could not resist trying the alternative approach to a precise measurement of the photon spectrum as pioneered by Haddock *et al.*<sup>11,12</sup> We report here a measurement of the neutron spectrum taken in coincidence with a photon. The analysis of this spectrum yields  $a_{nn} = -18.7 \pm 0.6$  fm and thus clearly supports our previous result from the photon spectrum.

The essential difference between the two methods can be illustrated with the help of Fig. 1, where kinematical contours are plotted for neutron versus photon energy. Though the photon energy ( $k$ ) is uniquely related to the relative momentum of the two neutrons in their center-of-mass system ( $p$ ), the most relevant range for the determination of  $a_{nn}$  ( $p \leq 25$  MeV/ $c$ ) is compressed into the last 0.62 MeV of the photon spectrum below the endpoint,

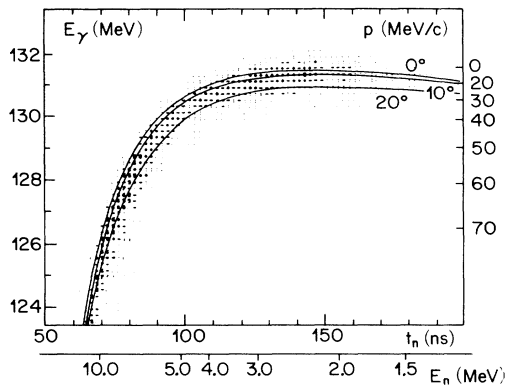


FIG. 1. Kinematical regions accepted by this experiment. The scatter plot shows Monte Carlo generated events accepted by the pair spectrometer (resolution 720 keV FWHM) and the corresponding time of flight of the coincident neutron. Kinematical loci for different photon-neutron angles are also shown.

as is evident from the relation

$$p^2 = m_n(Q - k) - k^2/4,$$

$$Q = m_\pi - (m_n - m_p) - B_d = 136.05 \text{ MeV}.$$

As we showed in our earlier paper, if  $a_{nn}$  is to be determined from the photon spectrum, one needs excellent energy resolution, a precise knowledge of the response function, and good stability of this response. On the other hand, for a coincidence experiment, if one restricts the photon-neutron angles to small values near back emission, neutrons with energies between 1.5 and 4.0 MeV all fall into the interesting region. Thus a moderate time-of-flight resolution and typical angular resolution suffice to give high resolution on the computed photon energy. Under the experimental conditions reported below, we obtained an equivalent photon energy resolution of 80 keV [full width at half maximum (FWHM)] compared to 720 keV (FWHM) with our earlier pair spectrometer measurement. This apparent advantage, however, is more than outweighed by the difficulties arising from the neutron detection. An accurately measured neutron counter efficiency is needed for low neutron energies. In addition, high background levels appear because of the low counter detection thresholds. These difficulties are clearly referred to and described in detail in the work of Haddock *et al.*<sup>11,12</sup> A rapid variation or large uncertainty of the neutron counter response in the range of 1.5–3.0 MeV neutron kinetic energy would cause a serious problem because the enhancement in the neutron spectrum due to the n-n-final state interaction is centered around 2.2 MeV. Figure 2 shows the sensitivity to  $a_{nn}$  in the region. Thus our present result must be viewed as a check of the  $\pi^-d \rightarrow nn\gamma$  technique for the extraction of  $a_{nn}$  with a completely different experimental setup and, consequently, with systematic errors which are drastically different from our previous experiment.

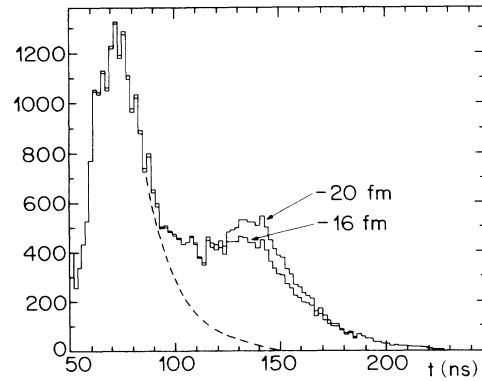


FIG. 2. Monte Carlo generated time-of-flight spectrum for events accepted within our apparatus for two different values of the neutron-neutron scattering length. The dashed curve shows the spectrum without final state interaction.

## II. EXPERIMENTAL DETAILS

The experiment was carried out in the  $\pi E1$  area of the SIN meson factory. A pion beam of 220 MeV/c momentum was brought to rest after proper degradation in a 8 cm long liquid deuterium target with a diameter of 6 cm. Photons from pion capture in deuterium were detected in either a pair spectrometer or an array of lead-glass Cerenkov counters, as shown in Fig. 3. The pair spectrometer, which has been described in detail elsewhere,<sup>6,13</sup> exhibits a resolution of 720 keV at the photon energy of the 129.4 MeV calibration line from the reaction  $\pi^-p \rightarrow n\gamma$  with pions at rest. Its acceptance is  $2.66 \times 10^{-5}$  with a 2.5% radiation length gold converter. The lead-glass detector consists of 49 modules, each with dimensions  $5.5 \times 5.5 \times 11 \text{ cm}^3$  and was placed 385 cm from the target. This detector has also been described previously.<sup>14</sup> It has an energy resolution  $\Delta E/E$  of 50%, a measured efficiency of 83% at 130 MeV, and thus an overall acceptance of  $6.6 \times 10^{-4}$ . Both detectors are insensitive to neutrons; charged particles are vetoed by scintillation counters covering their front. The pair spectrometer provides sufficient information so that one can reconstruct the origin of the photon in the target-beam plane and thus reject background from the beam defining scintillators and the target walls. For the lead-glass detector data this contribution has to be obtained from empty target data.

A double layer of ten plastic scintillators (NE110) with dimensions  $10 \times 100 \times 5 \text{ cm}^3$  was used as the neutron detector. Each bar is viewed by a photomultiplier tube on each end so that the vertical position of the neutron can be determined from the time difference (3.5 cm FWHM); the average flight time with respect to the pion arriving in the target can be measured with the sum of the photomultiplier signals (2 ns FWHM). The procedures necessary to set and maintain a constant detector threshold have been described by Tran *et al.*<sup>14</sup> These methods rely on  $^{137}\text{Cs}$ ,  $^{88}\text{Y}$ , and  $^{60}\text{Co}$   $\gamma$  sources and the known conversion of photon to proton light yields. We set the threshold at  $540 \pm 70$  keV proton energy. The neutron counter efficiency curve

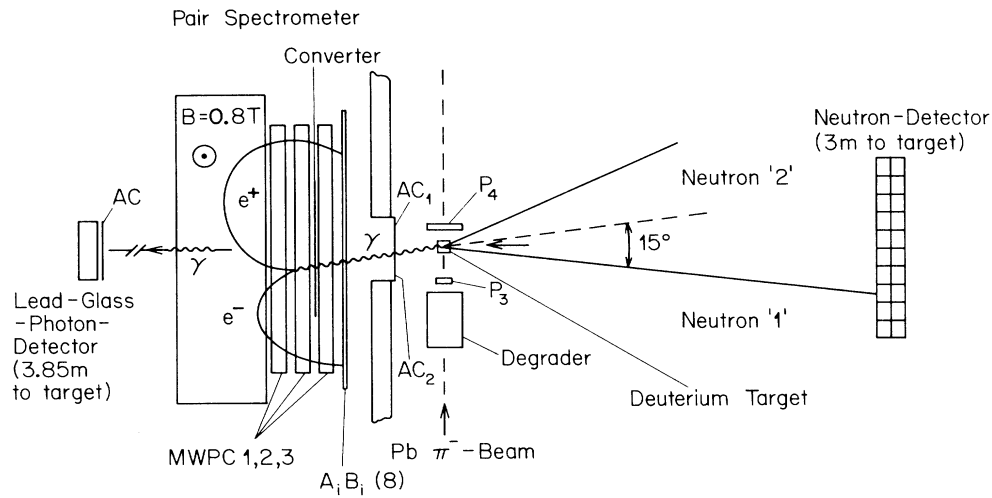


FIG. 3. Experimental setup used at SIN. Only the boundaries of the magnetic field region of the pair spectrometer are shown; the yoke is omitted.

is given in Fig. 4. It was determined in a separate experiment at the Lausanne University neutron generator.<sup>18</sup> A neutron beam of 2.6 MeV (14.1 MeV) was defined by detecting the  $^3\text{He}$  ( $^4\text{He}$ ) recoil nuclei from the reactions  $d(d,n)^3\text{He}$  [ $t(dn,n)^4\text{He}$ ] with 150 keV deuterons produced in a Van de Graaff accelerator. Subjecting the neutrons to a single scattering on free protons in a scintillator, the region between 0.5 and 2.2 MeV (4 and 8 MeV) was also covered. In this case the pulse height in the scintillator ensures scattering on free protons, while the time of flight and the scattering angle determine the neutron energy. The flux is obtained from the number of recoils and the known n-p cross section at low energy. A Monte Carlo program accounted for the number of neutrons scattered

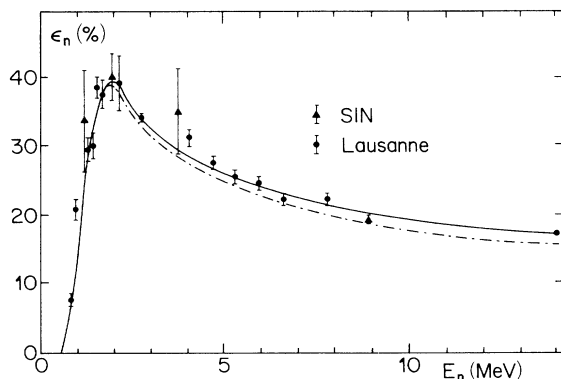


FIG. 4. Neutron counter efficiency vs neutron energy. The circular data points were measured with the Lausanne neutron generator; the triangular data points were obtained with pion capture in hydrogen and deuterium at SIN (see text). The solid curve represents a polynomial fit to the data points used in the analysis, whereas the dashed-dotted curve includes a correction for neutron scattering in the counters (see text).

out of the acceptance. Comparing the number of incident neutrons predicted by the Monte Carlo program to those actually detected gives the neutron counter efficiency. Another point on the efficiency curve was obtained using the  $\pi^-p \rightarrow n\gamma$  reaction, where an 8.8 MeV neutron can be tagged with the 129.4 MeV photon detected in the pair spectrometer. Three further points were determined from the two neutron events for  $\pi^-d \rightarrow nn\gamma$  reaction; these will be explained below. In the  $\pi^-p \rightarrow n\gamma$  case the number of detected neutrons was corrected for the probability that the neutron interacts in the hydrogen target or its walls (17%).

In Fig. 5 we show the raw neutron time-of-flight spectrum taken in coincidence with a photon detected in the pair spectrometer. It comprises the data of 66 h of running time with a primary beam intensity of  $3 \times 10^6 \pi^-/\text{s}$ . The hardware trigger in this run was given by the pair spectrometer only. In the analysis first all events with a photon reconstructed from multiwire proportional chamber data (see Refs. 6 and 13) were selected. The histogram of Fig. 5 then contains only the fraction, where a single neutron was detected in one of the front row neutron detectors with a time of flight within a 400 ns wide time window and valid neutron counter pulse height information. Only the first layer of the neutron detector was considered, because the scattering corrections of the first layer introduce too large an uncertainty for the treatment of the second layer data.

The time-of-flight window extends to unphysical times, i.e., flight times faster than valid for a photon and slower than valid for the lowest energy detectable neutrons. It is from these regions that the random background extending into the signal region is determined. This background has a time independent component from accelerator induced, but nonlocalizable background sources and a component from the degrader and the target correlated with the 50 MHz microstructure of the beam, i.e., a 20 ns repetition time. The data for the lead-glass detector were taken with

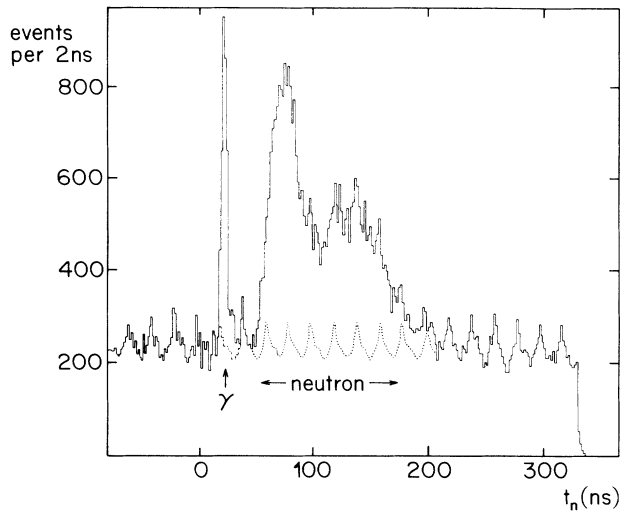


FIG. 5. Raw neutron time-of-flight spectrum taken in coincidence with a photon in the pair spectrometer. The dashed curves show the contribution from random coincidences determined from the data below 0 and above 240 ns neutron time of flight. The structure in the random contributions reflects the 50 MHz rf of the SIN accelerator (separation between consecutive beam bursts 20 ns).

a lower pion intensity ( $7 \times 10^5 \text{ s}^{-1}$ ) and during a period when the SIN accelerator ran with a 60 ns repetition cycle. The random background for these data was therefore about a factor of 2 smaller. Otherwise the neutron data were treated the same way.

The fact that we required only one neutron counter present in the coincidence leads to a small correction of the efficiency curve shown in Fig. 4, because when a neutron scatters from one detector into another with recoil protons detected in both the event is rejected. Below 1.6 MeV these cases are not detected, because the detector threshold is too high. At higher energies, the scattering of the neutrons from one detector to another can be accounted for by looking at those events in which the time-of-flight information of two counters is the same. These events form the majority of the two neutron events and are easily distinguishable from the two other contributions appearing in a two dimensional histogram of  $t_1$  (time of flight in the first counter) vs  $t_2$  (second counter). The band of the two neutron events from  $\pi^-d \rightarrow nn\gamma$  ( $t_1 + t_2 \cong 2t_0 = 296 \text{ ns}$ ) crosses the double scattering band ( $t_1 = t_2$ ) perpendicular near  $t_1 = t_2 = t_0$ , while the random two neutron events contribute a small background spread evenly over the whole histogram. Due to the energy dependence of the correction and due to differences in the amount of background encountered from one run to another, we first calculated a global efficiency, including those events which involve scattering and then determined a correction to this efficiency from the collected data themselves. Results are shown in Fig. 4 (dashed-dotted curve). A check of this correction is given by the 8.8 MeV point (neutrons from the reaction  $\pi^-p \rightarrow n\gamma$ ), which

was obtained rejecting events with more than one neutron counter firing. The background conditions for this point were nearly identical to the running conditions of the  $\pi^-d \rightarrow nn\gamma$  experiment.

After background subtraction, 40 000 (90 000) events remain from the pair spectrometer (lead-glass) data sample, which were compared to the theoretical models for the extraction of  $a_{nn}$ .

The small sample of true two neutron events (600 with a separation of at least one counter in between), however, allowed an autocalibration of the neutron counter efficiency. Since the direction and energy of one neutron determine the kinematics completely, the three-momentum of the second neutron can be predicted. The observed frequency distribution can be compared to the expected one taking into account neutron scattering in the target, thereby yielding the efficiency. The photon energy has been used to eliminate a large fraction of the random coincidences with a cut on the reconstructed  $Q$  value. Due to the limited statistics the data had to be grouped into three time intervals (90–135 ns, 2.6–6.0 MeV; 135–170 ns, 1.6–2.6 MeV; 170–220 ns, 1.0–1.6 MeV) with typical errors on the efficiency between 10% and 20%. These are plotted as triangles in Fig. 4.

### III. ANALYSIS AND RESULTS

In our previous paper we discussed in detail the similarities and differences between the various theoretical treatments<sup>16–21</sup> of the reaction  $\pi^-d \rightarrow nn\gamma$ . In particular, we have shown that all the corrections from higher partial waves, pion rescattering, etc., which are important at lower photon energies and higher relative neutron-neutron momenta, are negligible, if one limits the analysis to energies above 130 MeV ( $p \leq 35 \text{ MeV}/c$ ). Here only  $a_{nn}$  determines the shape of the spectrum. This is why we determined  $a_{nn}$  from a fit to the time-of-flight spectrum in the range 100–179 ns. The upper limit was chosen to avoid the region where the neutron counter efficiency varies rapidly. The particular theoretical ansatz used in the Monte Carlo simulation is due to de Téramond,<sup>20</sup> with a deuteron wave function determined from Reid soft-core potentials and a Yamaguchi parametrization of the  $n$ - $n$ -final state interaction. Event sets generated for different values of  $a_{nn}$  are subjected to the geometrical acceptances of the relevant detector setup, multiplied by the neutron counter efficiency, and finally the time of flight is smeared with the experimental resolution. Furthermore, the tiny variation of the pair spectrometer acceptance with energy<sup>6,13</sup> is considered as well as neutron scattering in the target. The latter effect is important. Typically 20% of all neutrons scatter at least once. However, since about 6 times as many neutrons are removed from the solid angle of the detector than are scattered into it, only 3% of the events in the spectrum arise from single scattering. However, if this effect is neglected, the result for  $a_{nn}$  would be altered by 2 fm.

Figures 6 and 7 show the time-of-flight spectra and the curves obtained from a fit of the Monte Carlo simulation to the data. Figure 6 includes all events from both data

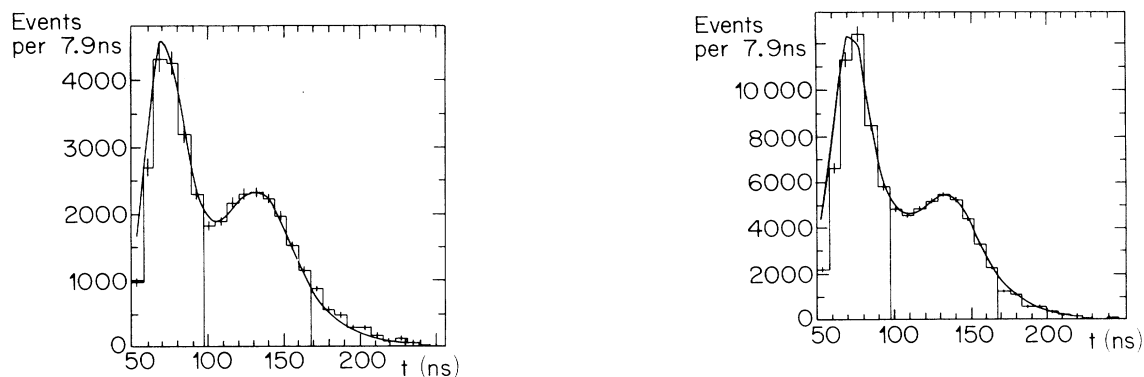


FIG. 6. Corrected neutron time-of-flight spectra (random coincidences eliminated) taken in coincidence with a photon in the pair spectrometer (left) and the lead-glass Čerenkov detector (right). The solid curves show the best fit to the data (in the region between the vertical lines) corresponding to  $a_{nn} = -18.4 \pm 0.8$  fm (left) and  $a_{nn} = -18.8 \pm 0.5$  fm (right).

sets, while the pair spectrometer data in Fig. 7 are subjected to a further cut on the measured photon energy. Only events above 130 MeV are included. This cut has no effect on the result from  $a_{nn}$ , except on the statistical error. The results are summarized in Table I. The principal contribution to the error is of statistical nature. The most important error source on the experimental side is the neutron counter response. The errors given correspond to a different parametrization of the efficiency curve that increases the chi square by one unit. Similarly, the error of the random background subtraction was included. The influence of the detector threshold was determined from a Monte Carlo simulation of the neutron counter efficiency.<sup>15</sup>

The theoretical uncertainties are given to indicate the sensitivity only. The error of 0.24 fm for pion rescatter-

ing corresponds to the change obtained in  $a_{nn}$ , if pion rescattering is completely neglected. Since the different theoretical treatments are in good agreement with each other, however (see Ref. 6), the true uncertainty is more likely to be around 0.05 fm. Similarly, the sensitivity to the deuteron  $d$ -state admixture given in Table I correspond to the case where no  $d$  state is retained. In our calculation we use 7%  $d$  state. Typically, the  $d$ -state contribution for alternative deuteron wave functions varies by  $\pm 2\%$  around this value. Hence, again, a negligible error arises from this quantity. An uncertainty of 0.02 fm was obtained for the shape of the deuteron wave function from a comparison of the two parametrizations Reid soft core<sup>22</sup> and McGee.<sup>23</sup>

Since the two data sets are statistically independent, we

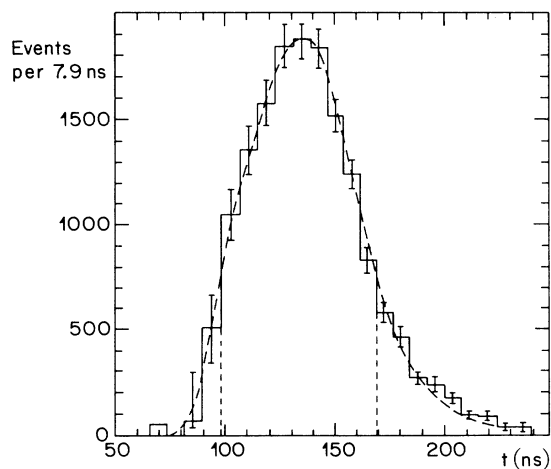


FIG. 7. Neutron time-of-flight spectrum taken in coincidence with a photon in the pair spectrometer with a measured energy above 130 MeV. The dashed line represents the fit to the data with  $a_{nn} = -18.3 \pm 1.1$  fm.

TABLE I. Summary of results.

Data set	$a_{nn}$ (fm)	$\chi^2/n_D$
Pair spectrometer	$-18.4 \pm 0.8$ (statistical)	1.1
Lead-glass array	$-18.8 \pm 0.5$ (statistical)	1.1
Final result <sup>a</sup>	$-18.7 \pm 0.6$	
Systematic errors		$\Delta a_{nn}$ (fm)
Shape of neutron counter efficiency curve	0.26	
Threshold setting ( $\pm 70$ keV)	0.20	
Absolute time of flight ( $\pm 0.5$ ns)	0.12	
Subtraction of background	0.16	
Geometrical acceptance ( $\gamma$ )	0.10	
Theoretical uncertainties		$\Delta a_{nn}$ (fm)
Pion rescattering	0.24	
Deuteron $d$ state	0.30	

<sup>a</sup>Weighted mean of two data sets (statistically), systematic effects, and theoretical errors added in quadrature.

quote the mean value of  $a_{nn} = -18.7 \pm 0.6$  fm as our final result. The statistical error of the mean has been increased by adding in quadrature the systematic errors, which are identical for both data sets.

#### ACKNOWLEDGMENTS

This work has been supported by SIN, the Swiss National Science Foundation, and the German Bundesministerium for Science and Technology.

\*Present address: Centre Information, Université de Lausanne, CH-1015 Lausanne, Switzerland.

†Present address: RANK XEROX, CH-1015 Lausanne, Switzerland.

<sup>1</sup>R. H. Phillips and K. M. Crowe, *Phys. Rev.* **96**, 484 (1954).

<sup>2</sup>M. N. McNaughton *et al.*, in *Few Particle Problems in the Nuclear Interaction*, edited by I. Slaus *et al.* (North-Holland, Amsterdam, 1972), p. 108.

<sup>3</sup>W. Breunlich, S. Tegesen, W. Bertl, and A. Chalupka, *Nucl. Phys.* **A221**, 269 (1974).

<sup>4</sup>B. Zeitnitz, R. Maschuw, P. Suler, W. Ebenhöf, J. Bruinsma, and J. H. Stuivenberg, *Nucl. Phys.* **A231**, 13 (1974).

<sup>5</sup>W. von Witsch, B. Gomez Moreno, W. Rosenstock, K. Ettl, and J. Bruinsma, *Phys. Lett.* **80B**, 187 (1979); *Nucl. Phys.* **A329**, 141 (1979).

<sup>6</sup>B. Gabioud *et al.*, *Nucl. Phys.* **A420**, 496 (1984); *Phys. Rev. Lett.* **42**, 1508 (1979); *Phys. Lett.* **103B**, 9 (1981).

<sup>7</sup>J. L. Friar and B. F. Gibson, *Phys. Rev. C* **17**, 1752 (1978); S. A. Coon, M. D. Scadron, and P. C. McNamee, *Nucl. Phys.* **A287**, 381 (1977); **A249**, 483 (1975); R. A. Brandenburg, S. A. Coon, and P. U. Sauer, *ibid.* **A294**, 905 (1978).

<sup>8</sup>A. W. Thomas, *Adv. Nucl. Phys.* **13**, 1 (1983).

<sup>9</sup>M. D. Miller, M. S. Sher, P. Signell, N. R. Yoder, and D. Marker, *Phys. Lett.* **30B**, 157 (1969).

<sup>10</sup>I. Slaus, Y. Akaishi, and H. Tanaka, *Phys. Rev. Lett.* **48**, 993 (1982).

<sup>11</sup>R. W. Salter, R. P. Haddock, Z. Zeller, D. R. Nygren, and J. B. Czirr, *Nucl. Phys.* **A254**, 241 (1975).

<sup>12</sup>R. P. Haddock, R. M. Salter, M. Zeller, J. B. Czirr, and D. R. Nygren, *Phys. Rev. Lett.* **14**, 318 (1965).

<sup>13</sup>J. C. Alder *et al.*, *Nucl. Instrum. Methods* **160**, 93 (1978).

<sup>14</sup>M. T. Tran *et al.*, *Nucl. Phys.* **A324**, 301 (1979).

<sup>15</sup>See O. Schori, Ph.D. thesis, Université de Lausanne, 1985.

<sup>16</sup>K. M. Watson and R. N. Stuart, *Phys. Rev.* **32**, 738 (1951).

<sup>17</sup>K. W. McVoy, *Phys. Rev.* **121**, 1401 (1961).

<sup>18</sup>M. Bander, *Phys. Rev.* **134**, B1052 (1964).

<sup>19</sup>W. R. Gibbs, B. F. Gibson, and G. J. Stephenson, Jr., *Phys. Rev. C* **11**, 90 (1975); **12**, 2130 (1975); **16**, 322 (1977); **17**, 356 (1978).

<sup>20</sup>G. F. de Téraumont, *Phys. Rev. C* **16**, 1976 (1977).

<sup>21</sup>G. F. de Téraumont, J. Paez, and C. W. Soto Vargas, *Phys. Rev. C* **21**, 2542 (1980).

<sup>22</sup>R. V. Reid, *Ann. Phys. (N.Y.)* **50**, 411 (1968).

<sup>23</sup>I. J. McGee, *Phys. Rev.* **151**, 772 (1966).